SUPPLEMENTAL INFORMATION

CCR1 BLOCKADE REDUCES TUMOR BURDEN AND OSTEOLYSIS IN VIVO IN A MOUSE MODEL OF MYELOMA BONE DISEASE

Dairaghi et al.

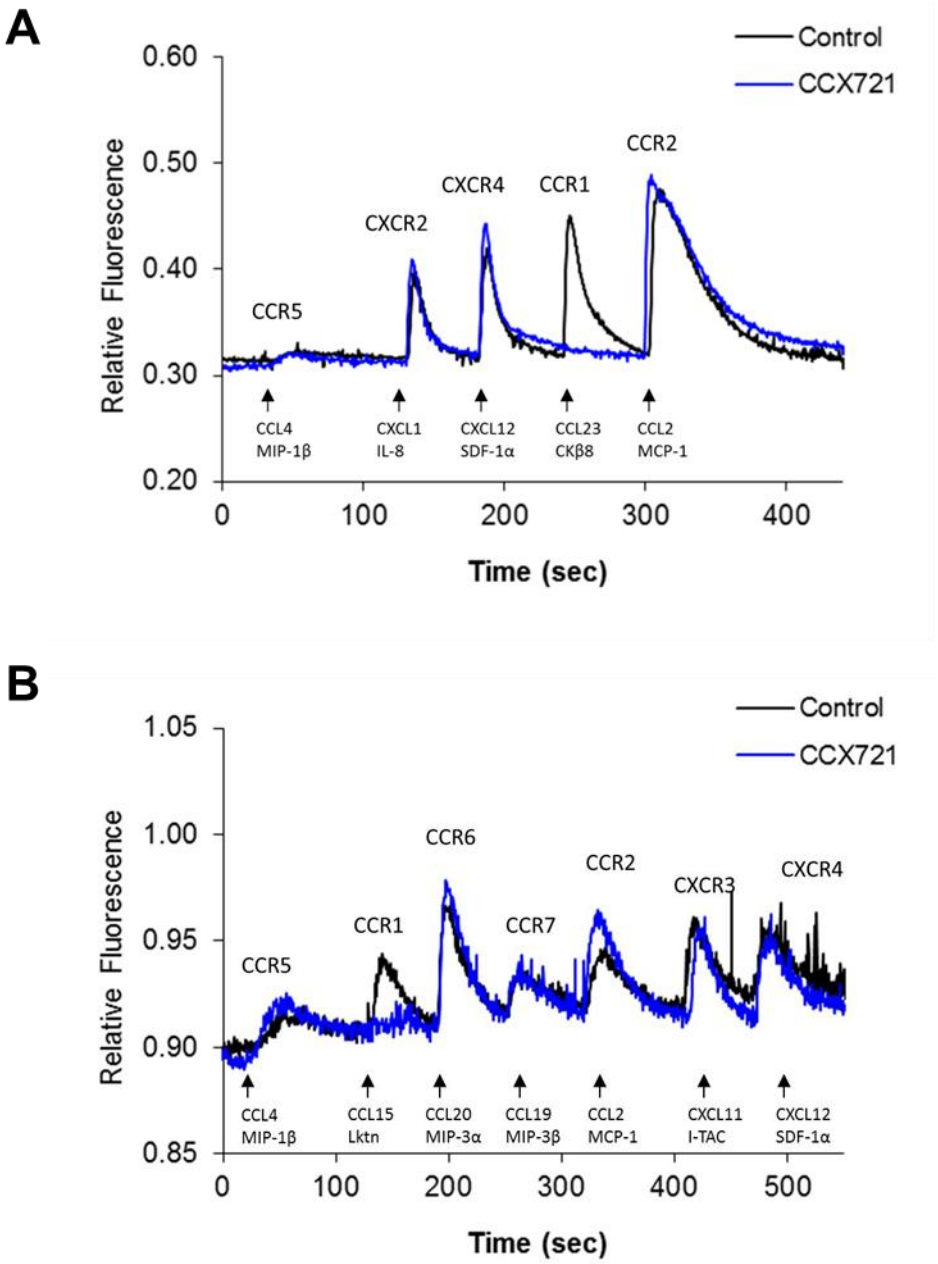

Supplemental Figure 1. Specificity of CCX721 for CCR1 over other chemokine receptors. Human monocytes **(A)** or lymphocytes **(B)**, labeled with the fluorescent indicator dye Indo-1 AM, were tested for functional responses to various chemokines, either in the presence or absence of CCX721. In these graphs, the elapsed time is shown along the x-axis and the relative fluorescence (410 nm / 490 nm ratio) is shown on the y-axis. CCX721, added to 10 µM at 5 seconds, is shown in blue, and the control, DMSO added to 0.1% at 5 seconds, in black. Chemokines were added in a sequential manner, with the chemokine listed below the trace and the corresponding receptor listed above. **(A)** Data with freshly isolated human monocytes; CCL4 was added to a final concentration of 50 nM, and the other chemokines were added at 5 nM. **(B)** Data with cultured human lymphocytes; chemokines were added at a final concentration of 10 nM.

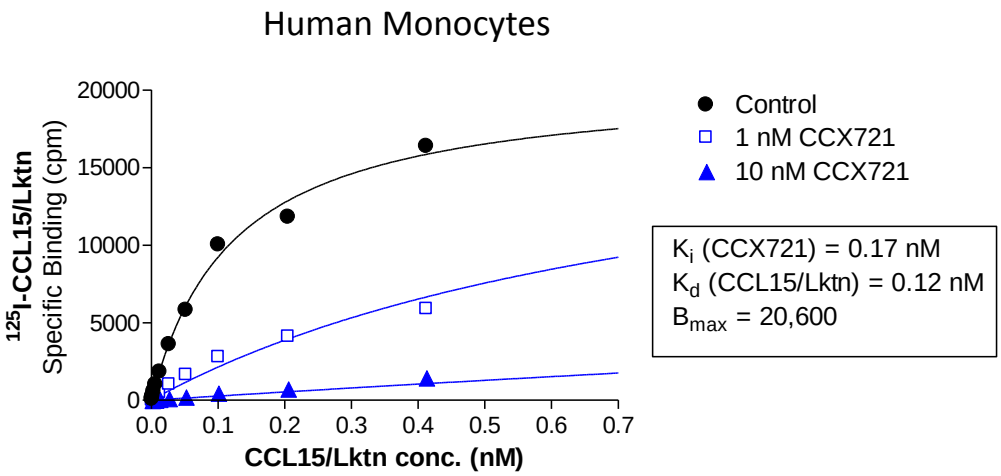

Supplemental Figure 2. CCX721 potently inhibits specific binding of a radiolabeled chemokine to monocyte-expressed CCR1. The specific binding of ^{125}I-labeled CCL15 to freshly isolated human monocytes was determined using the difference of binding alone and in the presence of a >100-fold excess of unlabeled CCL15 for each concentration of [^{125}I]-CCL15 tested. The control results (black circles) and those in the presence of 1 nM (open blue squares) and 10 nM (blue triangles) CCX721 are shown. The potency of CCX721 (K_i) and CCL15 (K_d) was determined using the equation K_d-apparent = K_d x (1 + [CCX721]/K_i) and global fit parameters with Graphpad Prism software (La Jolla, CA)

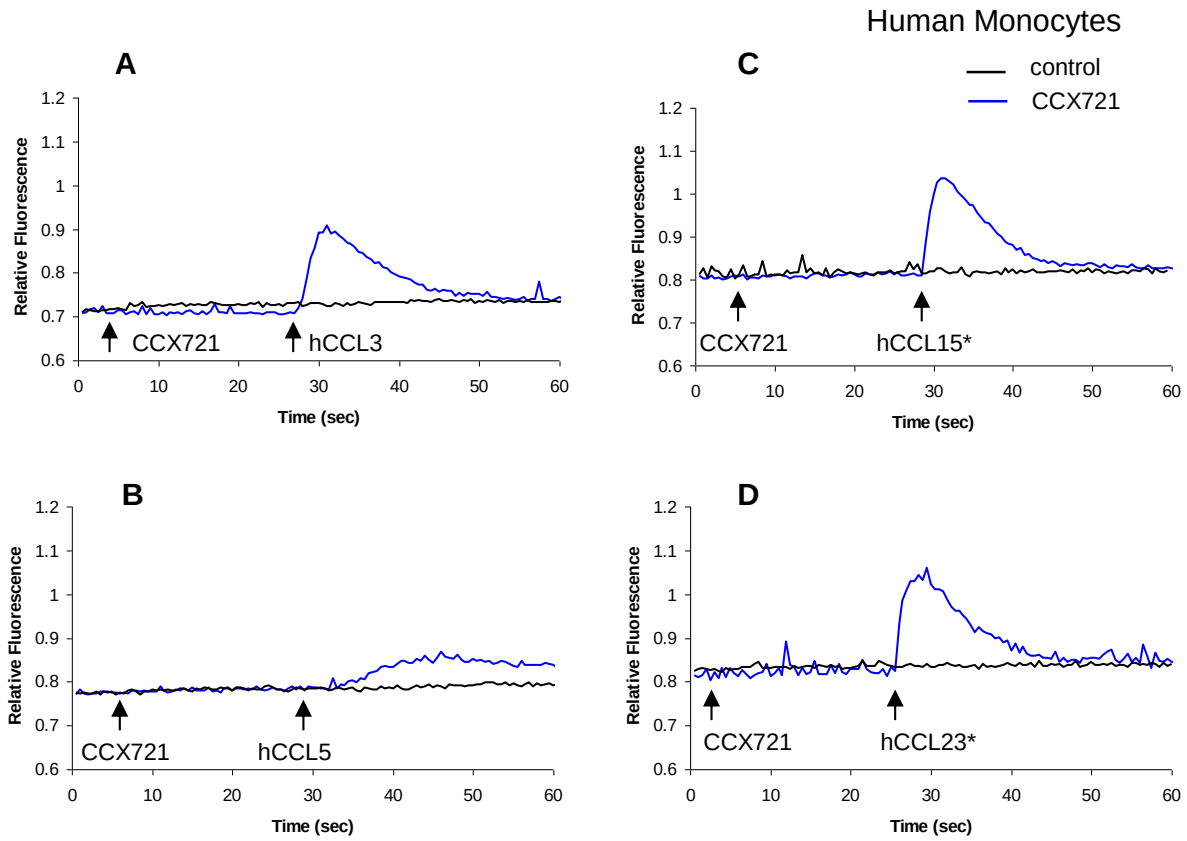

Supplemental Figure 3. All chemokine agonists of CCR1 are inhibited by CCX721. Freshly isolated human monocytes, labeled with the fluorescent indicator dye Indo-1 AM, were tested for functional responses to CCR1 chemokines either in the presence or absence of CCX721. In this graph, the elapsed time is shown along the x-axis and the relative fluorescence (410 nm / 490 nm ratio) is shown on the y-axis. CCX721, added to 100 nM at 5 seconds, is shown in black, and the control, DMSO added to 0.1% at 5 seconds, in blue. Chemokines were added to 10 nM, with the specific chemokine added listed below the trace. Asterisk denotes the "super-agonist" N-terminal truncated forms of the chemokines CCL15 and CCL23 (Berahovich et al., J Immunol. 2005; 174:7341).

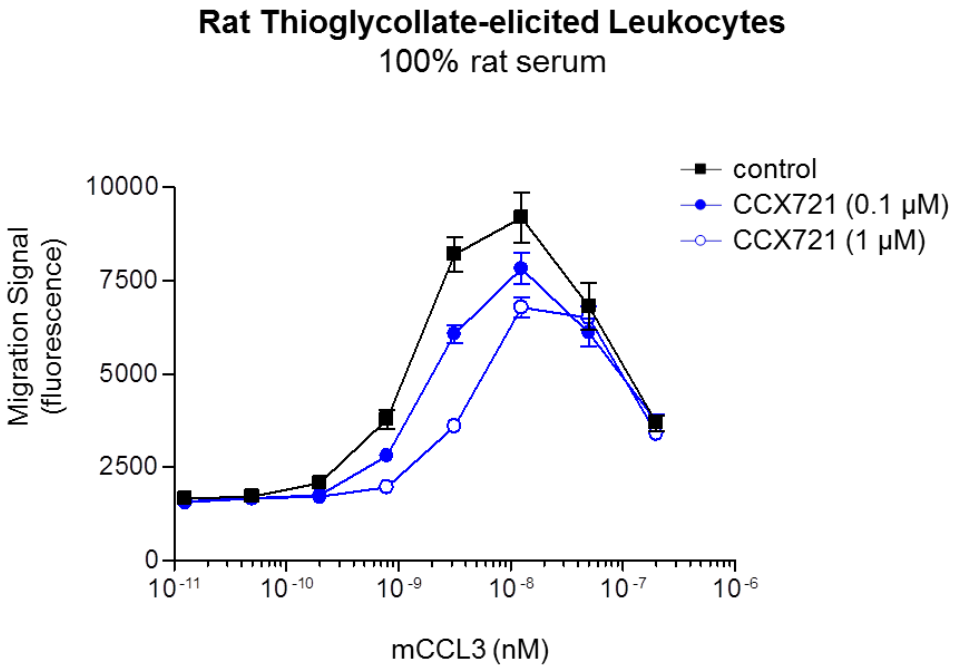

Supplemental Figure 4. Potency of CCX721 toward rat CCR1 in a chemotaxis assay conducted in rat serum. The chemotactic response of freshly isolated rat leukocytes, isolated by lavage from thioglycolate-elicited peritoneal cells and resuspended in rat serum, was measured in response to increasing concentrations of rodent CCL3; the migration signal is shown along the y-axis. Comparison of the control-treated (DMSO added to 0.2%) and CCX721-treated groups using the standard dose-ratio equation of pA_2 = p[CCX721(M)] – p[(A'/A)-1] where A reflects the control potency and A' the potency of the agonist in the presence of CCX721.

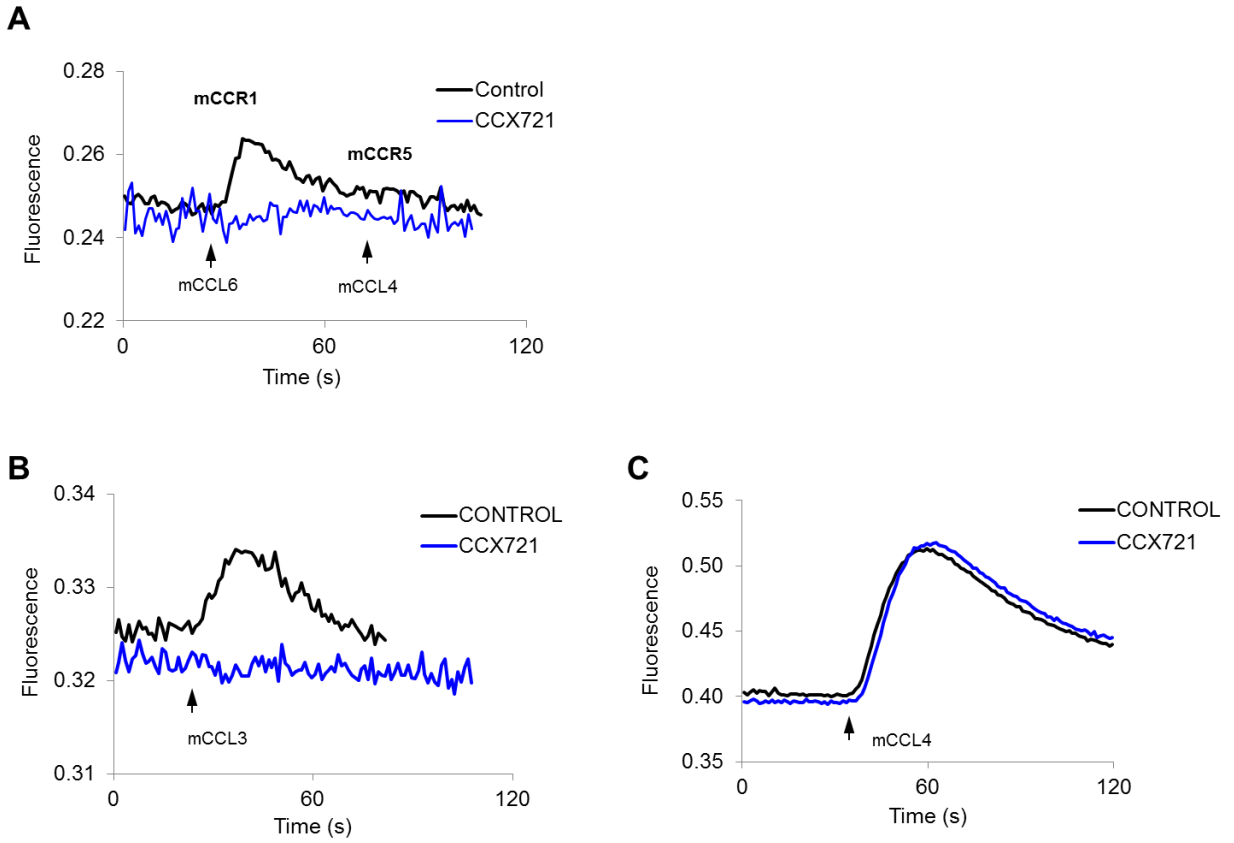

Supplemental Figure 5. Expression of CCR1 on mouse bone marrow monocytes and selective inhibition of mouse CCR1, but not mouse CCR5, by CCX721. Mouse monocytes, defined as being CD11b-positive and Ly-6G-negative, were isolated by negative selection from C57BL/6 bone marrow with a monocyte enrichment kit (STEMCELL Technologies, Vancouver, Canada), with >85% purity achieved, as measure by flow cytometry with antibodies to mouse CD11b and Ly-6G (BD Biosciences, San Jose, CA). **(A)** After labeling with Indo-1 AM, these cells released calcium from intracellular stores in response to the mouse CCR1-active chemokine mCCL6/C10 (Berahovich et al., J Immunol. 2005; 174:7341), but not in response to the CCR5-active chemokine mCCL4. The CCR1-mediated signal was completely inhibited in the presence of 10 µM CCX721. **(B)** With the mouse monocytic WEHI cell line (ATCC, Rockville, MD), addition of CCX721 to 1 µM completely blocked mouse CCR1-mediated calcium flux, mediated by addition of 50 nM mCCL3. **(C)** Conversely, addition of CCX721 to 10 µM had no effect upon mouse CCR5-mediated calcium flux, mediated by addition of 1 nM mCCL4 to mCCR5-transfected L1.2 cells.

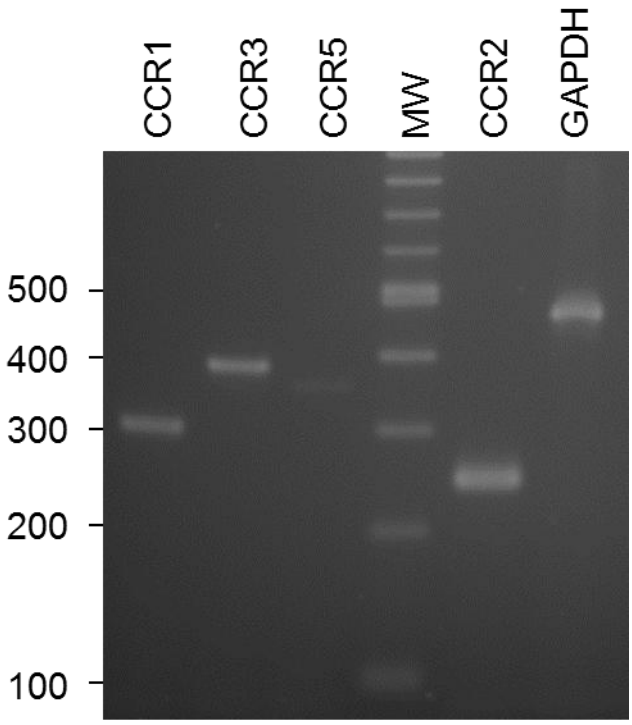

Supplemental Figure 6. Expression of chemokine receptors CCR1, CCR2, CCR3 and CCR5 by monocytes isolated from mouse bone marrow. A negative selection kit (StemCell Technologies; Vancouver, Canada) was used to isolate bone marrow monocytes from C57BL/6 mice, resulting in a purity of >85% as measured by flow cytometry using monoclonal antibodies to CD11b and Ly-6G surface markers. RT-PCR was conducted with primers specific for murine CCR1, CCR2, CCR3 and CCR5, and the results are shown, alongside molecular weight markers, in an agarose gel.

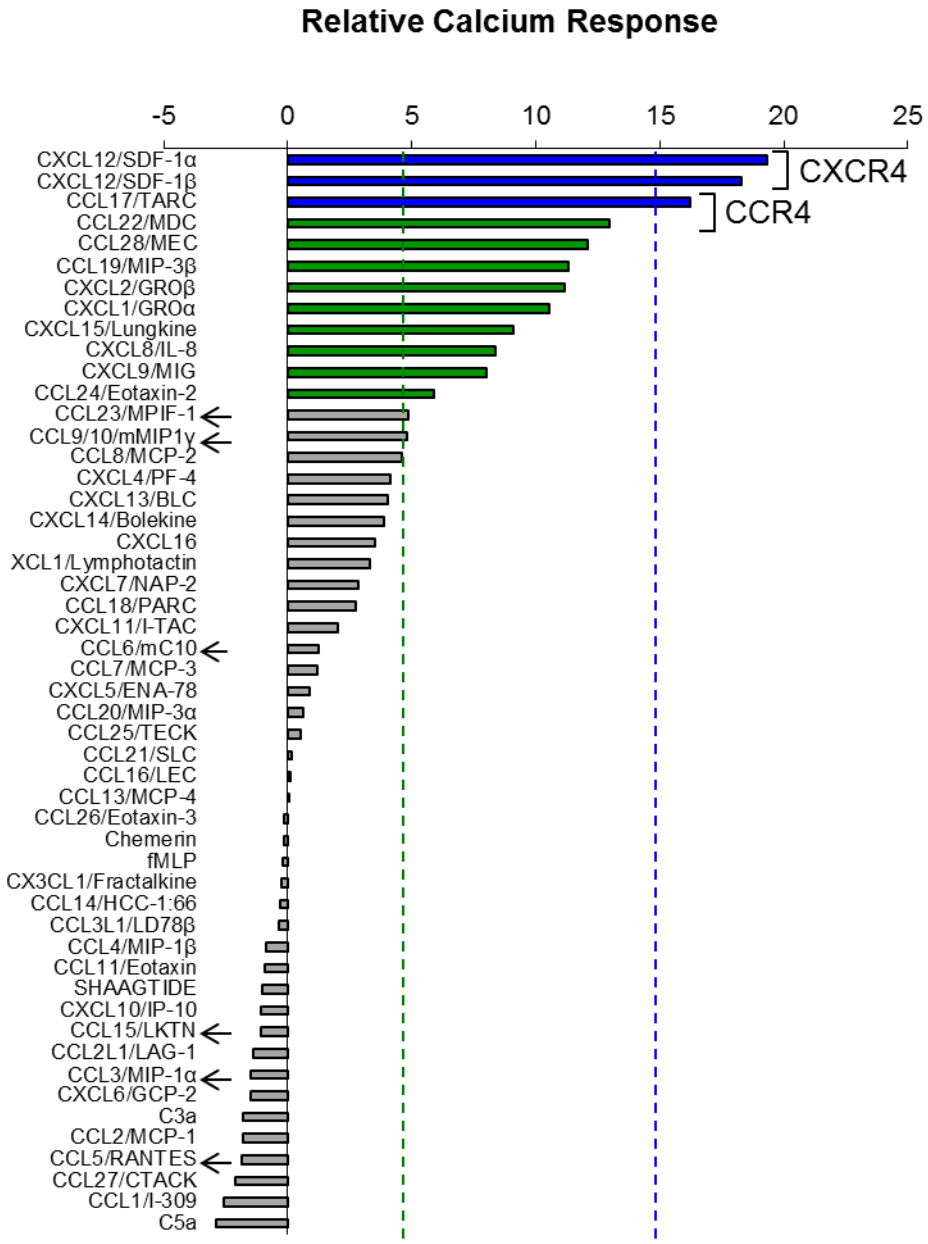

Supplemental Figure 7. Characterization of 5TGM-GFP functional responses to chemokine stimulation. Fifty-one chemokines, or related proteins, were added to a final concentration of 1 µg/mL, with n=4 replicates, to 5TGM-GFP cells labeled with the fluorescent indicator dye Calcium-4 on the Fluorescent Imaging Plate Reader (FLIPR), and changes in fluorescent signal, indicative of changes in cytoplasmic calcium mobilization, were measured over a two minute time course. The Relative Calcium Response for each protein was normalized to that of added vehicle (0%) or ionomycin (100%), where a value from -5% to 5% is considered “no response” (grey bars), from 5% to 15% is a “weak response” (green bars), and from 15% to 50% is a “moderate response” (blue bars). Proteins are listed along the y-axis, ranked by their effect (strongest to weakest), and those that are CCR1 agonists are marked by an arrow. The strongest responses were obtained by stimulation of CXCR4 and CCR4 chemokine receptors.

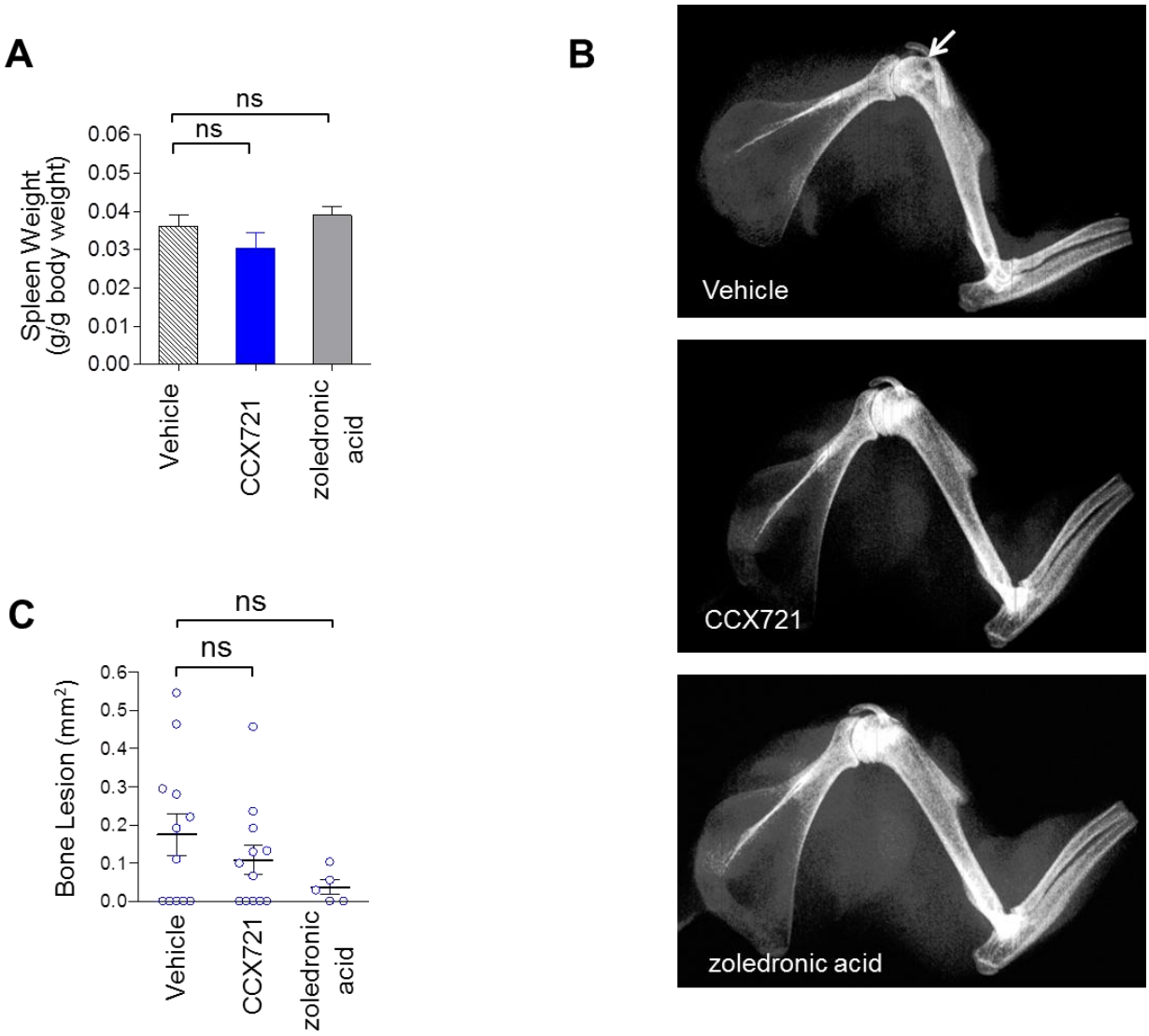

Supplemental Figure 8. Prophylactic treatment with CCX721 or zoledronic acid in the 5TGM1 tumor model – effects on spleen weight and osteolytic lesions. After 28 days of treatment (study day 28), animals were weighed, euthanized, spleens harvested and radiographs of fixed bone taken. **(A)** Organ weight, normalized by body weight, is shown for each treatment group (mean ± SEM). **(B)** Representative radiographs of upper limbs. Radiographs of fixed bones were obtained using a Faxitron radiographic inspection unit (Kodak, Rochester, NY)[32]. The arrow (upper panel, vehicle-treated 5TGM1 tumor-bearing mice) indicates an osteolytic lesion (radiolucent area in metaphyseal region) visible on humerus. **(C)** Areas of osteolytic bone lesions, recognized as well-circumscribed radiolucent lesions on radiographs, were quantitated using MetaMorph imaging software (Molecular Devices, Downingtown, PA). Radiographs were analyzed by investigators blinded to the composition of the groups or the experimental protocol. Area data for each group are presented as mm^2/lesion (mean ± SEM). ns, not significant ($p>0.05$) by Mann-Whitney test.

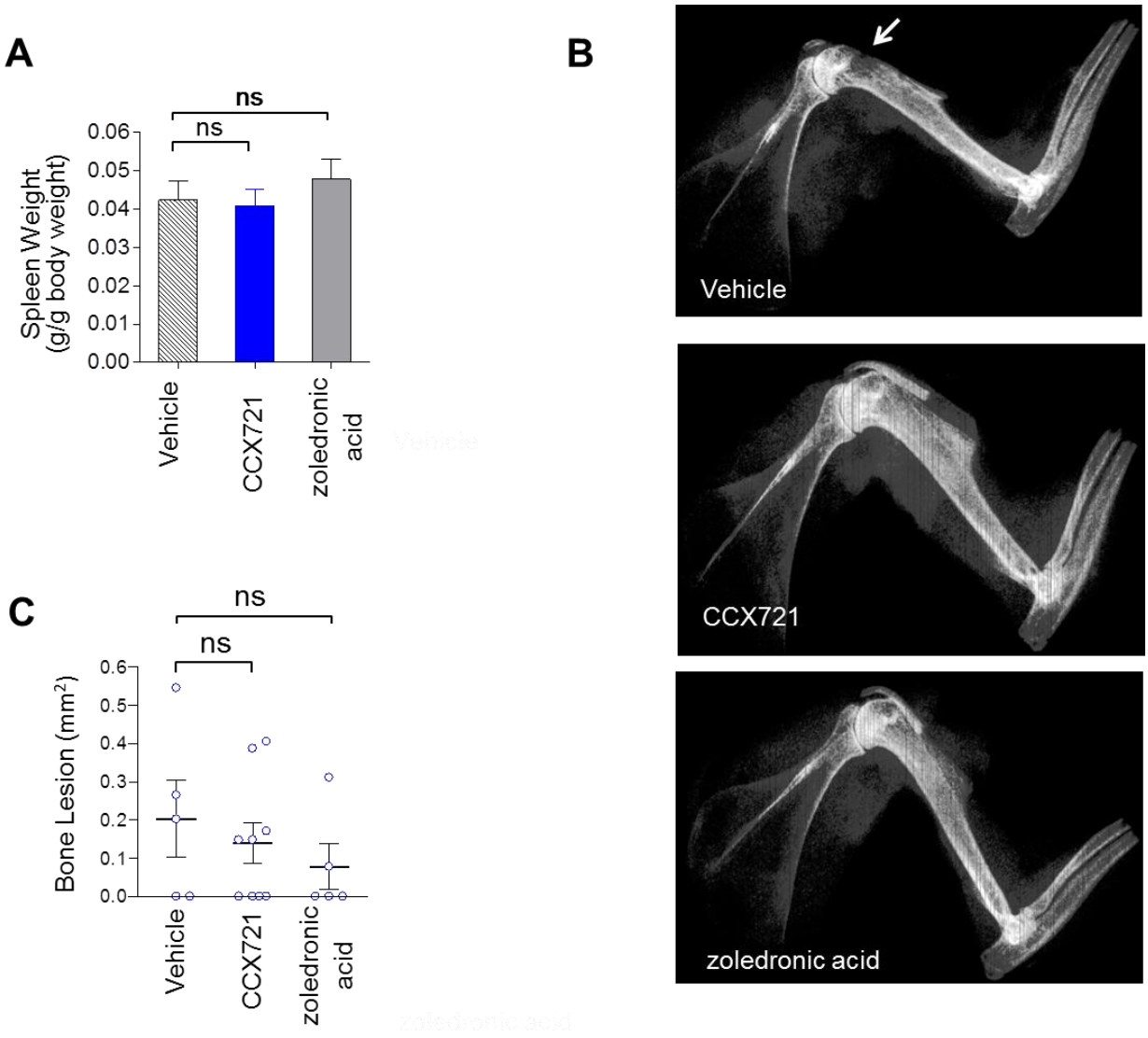

Supplemental Figure 9. Therapeutic treatment with CCX721 or zolendronic acid in the 5TGM1 tumor model – effects on spleen weight and osteolytic lesions. After 10 days of treatment (study day 28), animals were weighed, euthanized, spleens harvested and radiographs of fixed bone taken. **(A)** Organ weight, normalized by body weight, is shown for each treatment group (mean ± SEM). **(B)** Representative radiographs of upper limbs. Radiographs of fixed bones were obtained using a Faxitron radiographic inspection unit (Kodak, Rochester, NY)[32]. The arrow (upper panel, vehicle-treated 5TGM1 tumor-bearing mice) indicates an osteolytic lesion (radiolucent area in metaphyseal region) visible on humerus. **(C)** Areas of osteolytic bone lesions, recognized as well-circumscribed radiolucent lesions on radiographs, were quantitated using MetaMorph imaging software (Molecular Devices, Downingtown, PA). Radiographs were analyzed by investigators blinded to the composition of the groups or the experimental protocol. Area data for each group are presented as mm^2/lesion (mean ± SEM). ns, not significant ($p>0.05$) by Mann-Whitney test.

From Fig. 3C

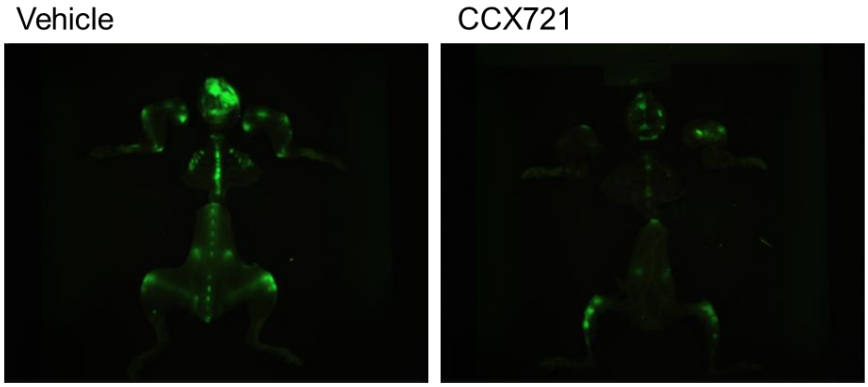

From Fig. 4C

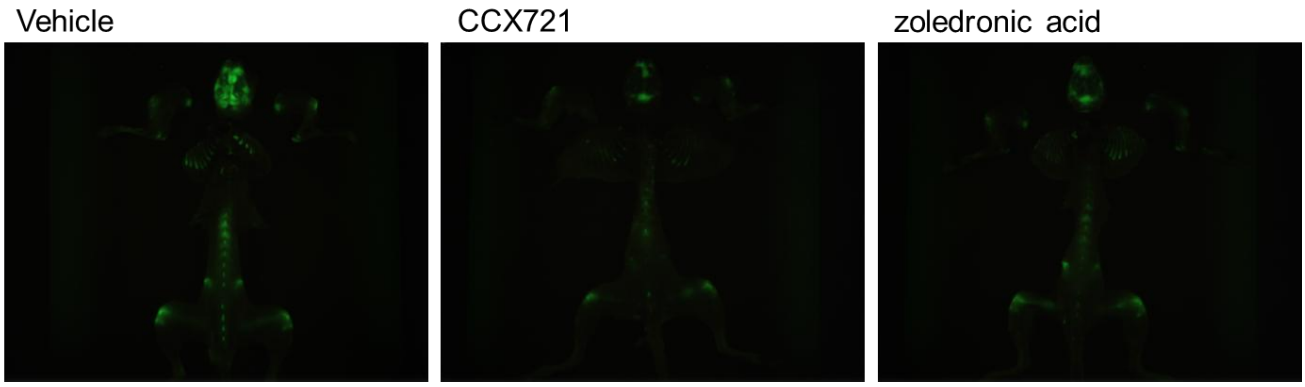

Supplemental Figure 10. Whole animal GFP images, original coloration, from Fig. 3C and Fig. 4C.

Supplemental Table 1. Selectivity profile of CCX721 against a panel of chemokine receptors and other biologically important targets.

Receptor	Cell Type	Agonist	Assay	IC_{50}
CCR2	Human lymphocytes	CCL2	Ca^{2+} flux	>10 μM
	THP-1	CCL2	Chemotaxis	>10 μM
CCR5	Human lymphocytes	CCL4	Ca^{2+} flux	>10 μM
	Baf3-CCR5	CCL4	Chemotaxis	>10 μM
mCCR5	Baf3-mCCR5	mCCL4	Chemotaxis	>10 μM
CCR6	Human lymphocytes	CCL20	Ca^{2+} flux	>10 μM
CCR7	Human lymphocytes	CCL19	Ca^{2+} flux	>10 μM
CXCR3	Human lymphocytes	CXCL11	Ca^{2+} flux	>10 μM
CXCR4	Human lymphocytes	CXCL12	Ca^{2+} flux	>10 μM
ChemR23	Baf3 ChemR23	hC9 peptide	Chemotaxis	>10 μM

Receptor	Family	CCX721 test concentration	Inhibition
A_1	Adenosine	10 μM	30%
A_{2A}	Adenosine	10 μM	6%
A_3	Adenosine	10 μM	35%
$alpha_1$ (non-selective)	Adrenergic	10 μM	4%
$alpha_2$ (non-selective)	Adrenergic	10 μM	-15%
$beta_1$	Adrenergic	10 μM	7%
$beta_2$	Adrenergic	10 μM	9%
AT_1	Angiotensin-II	10 μM	-13%
BZD (central)	GABA	10 μM	-5%
B_2	Bradykinin	10 μM	-6%
CB_1	Cannabinoid	10 μM	-4%
CCK_A (CCK_1)	Cholecystokinin	10 μM	1%
D_1	Dopamine	10 μM	0%
D_{2S}	Dopamine	10 μM	-1%
ET_A	Endothelin	10 μM	-2%
GABA (non-selective)	GABA	10 μM	-1%
GAL_2	Galanin	10 μM	2%
CXCR2 (IL-8B)	Chemokine	10 μM	-2%
H_1	Histamine	10 μM	5%
H_2	Histamine	10 μM	14%
MC_4	Melanocortin	10 μM	-5%
MT_1	Melatonin	10 μM	-2%
M_1	Muscarinic	10 μM	14%

Receptor	Family	CCX721 test concentration	Inhibition
M_2	Muscarinic	10 µM	-5%
M_3	Muscarinic	10 µM	-6%
NK_2	Neurokinin	10 µM	4%
NK_3	Neurokinin	10 µM	10%
Y_1	Neuropeptide Y	10 µM	-3%
Y_2	Neuropeptide Y	10 µM	11%
NT_1 (NTS_1)	Neurotensin	10 µM	-12%
$delta_2$ (DOP)	Opioid & opioid-like	10 µM	6%
kappa (KOP)	Opioid & opioid-like	10 µM	-1%
mu (agonist site) (MOP)	Opioid & opioid-like	10 µM	3%
ORL1 (NOP)	Opioid & opioid-like	10 µM	-5%
TP (TXA2/PGH2)	Prostanoid	10 µM	11%
5-HT_{1A}	Serotonin	10 µM	-5%
5-HT_{1B}	Serotonin	10 µM	20%
5-HT_{2A}	Serotonin	10 µM	-1%
5-HT_3	Serotonin	10 µM	-8%
5-HT_{5A}	Serotonin	10 µM	2%
5-HT_6	Serotonin	10 µM	6%
5-HT_7	Serotonin	10 µM	-5%
sst (non-selective)	Somatostatin	10 µM	11%
VIP_1 ($VPAC_1$)	Vasoactive Intestinal Peptide	10 µM	1%
V_{1a}	Vasopressin	10 µM	-12%
Ca^{2+} channel (L, verapamil site) (phenylalkylamines)	Calcium (Ca^{2+}) channel	10 µM	13%
K_V channel	Potassium (K^+) channel	10 µM	-9%
SK_{Ca} channel	Potassium (K^+) channel	10 µM	8%
Na^+ channel (site 2)	Sodium (Na^+) channel	10 µM	4%
Cl^- channel	Chlorine (Cl^-) channel	10 µM	13%
hERG	Potassium (K^+) channel	0.4 µM	2%
hERG	Potassium (K^+) channel	0.7 µM	6%
hERG	Potassium (K^+) channel	1.2 µM	15%
hERG	Potassium (K^+) channel	2.4 µM	32%
hERG	Potassium (K^+) channel	5.8 µM	54%
NE transporter	Norepinephrine transporter	10 µM	-14%
DA transporter	Dopamine transporter	10 µM	12%
5-HT transporter	Serotonin transporter	10 µM	82%

Assay	**Substrate**	**IC_{50}**
CYP 1A2	Phenacetin	40 µM
CYP 2C9	Diclofenac	19 µM
CYP 2C19	(S)-Mephenytoin	>50 µM
CYP 2D6	Bufuralol	>50 µM
CYP 3A4	Midazolam	>50 µM
	Testosterone	38 µM